

## Review

### Semi-classical Methods in Non-Sequential Double Ionization

Allan S. Johnson, André Staudte and D. M. Villeneuve\*

*Joint Attosecond Science Laboratory,  
National Research Council of Canada and University of Ottawa,  
100 Sussex Drive,  
Ottawa ON K1A 0R6, Canada  
(Received September 17, 2013)*

Non-sequential double ionization of an atom in an intense laser field is a prototypical problem in multi-body strong field interactions. To examine non-sequential double ionization, an often used approach is the semi-classical method, by which initial conditions are set according to quantum expressions and the ensuing dynamics modelled classically. Here we present a comparative study of quantum and semi-classical methods in the single active electron approximation. We show that semi-classical methods over-estimate the kinetic energy of rescattered electrons by up to 150%. We further show that the return time of the recolliding electrons deviates between quantum and semi-classical methods at low intensities, and that the deviation is attributable to the choice of the initial tunnelling position.

DOI: 10.6122/CJP.52.329

PACS numbers: 71.27.+a, 73.23.Hk, 34.80.Dp

## I. INTRODUCTION

The three step model of electron recollision in strong laser fields has become one of the linchpins of strong field physics [1, 2]. In its canonical formulation, an electron tunnels out of an atom or molecule in the presence of a strong laser field, propagates in the presence of said field, and finally returns with a kinetic energy of up to  $3.17U_p + I_p$ , where  $U_p$  is the ponderomotive potential of the field and  $I_p$  is the ionization potential [3]. While the three step model has been tremendously successful, explaining high harmonic generation and angular structure in above threshold ionization electrons, only recently has the three step model moved significantly outside the single active electron approximation, with new models for rescattering in complex systems [4]. The notable exception is non-sequential double ionization (NSDI) [5–7], which forms a prototypical multi-body strong field problem [8]. Here, the recolliding electron causes a second electron to detach in a highly correlated process. This is thought to proceed by a variety of mechanisms, including ‘knock-out’ e-2e collisions [9, 10], recollision excitation with subsequent ionization (RESI) [11, 12], and formation of transient doubly excited states [13, 14]. NSDI was one of the earliest successes of the 3 step model, and has accordingly been thoroughly studied for over ten years, and

---

\*Electronic address: david.villeneuve@nrc.ca

great success has been obtained treating the problem with semi-classical methods [4]. Semi-classical methods are widely used, as full quantum treatments are extremely computational demanding and have thusfar only been possible at wavelengths of 400nm, while almost all experiments have been performed at 800 nm [15]. Semi-classical methods begin by setting initial conditions according to a mixture of analytic quantum theories and statistical ensembles [8], and then propagating the system using classical mechanics. These models have successfully recreated such features of NSDI as the enhanced probability [16], recoil ion momenta distributions [17], and electron correlation patterns [18].

Despite these successes, the problem of NSDI is far from completely understood. Recent studies have shown a variety of interesting new phenomena not previously observed, including new effects occurring at low intensities [19, 20] and modified correlation spectra with single cycle laser pulses [12, 14]. While one might expect these new phenomena to require a more complete quantum treatment as the effects of cycle averaging are removed and the energy of the recolliding electron decreases below the threshold for ionization, thus far semi-classical modelling has been sufficient to describe most of the observed effects [14, 16, 21, 22]. This raises the interesting question of when semi-classical methods can be expected to fail, if not when intuitively it would seem the quantum structure of the ion would dominate dynamics. To that effect, we have performed a comparative examination between full quantum and semi-classical models for the first two steps of NSDI - ionization and propagation of the first electron. By examining the kinematics of the recolliding electron, we identify when the quantum structure of the target is likely to influence NSDI. Incredibly, we find that despite its successes, semi-classical models deviate significantly from a full quantum treatment across a broad range of conditions. In particular, semi-classical methods systematically over-estimate the maximum recollision energy of the electron at low intensities by up to a maximum of 150%. Furthermore, at low intensities the time of recollision is also incorrectly modelled by the semi-classical method, leading to recollision taking place in the presence of a strong field instead of around a zero-crossing. Our results suggest that semi-classical methods must be looked at carefully when used to model NSDI at low intensities.

## II. METHODS

In order to compare semi-classical methods with a full quantum treatment and to be able to present the results clearly, we perform simulations in the one dimensional, single active electron approximation. It is straightforward to use fully 3D classical calculations, and 3D quantum calculations. However the essence of what we are trying to demonstrate can most easily be seen in 1D.

Semi-classical methods employ Newton's equations to predict the trajectory of electrons in the presence of a Coulomb potential (due to the ion) and of a time-varying electric field in the dipole approximation (due to the laser field). For intensities below  $10^{16}$  W/cm<sup>2</sup>, the magnetic field associated with the laser field can be neglected. Several approximations must be made; for example, the singularity associated with the Coulomb potential leads

to unrealistic accelerations and velocities, and a softened potential is used [23, 24]. The electron can quantum-mechanically tunnel through the potential barrier, even though it does not have sufficient energy to do so classically; therefore in semi-classical calculations the electron must be placed outside the barrier at a position that mimics the position at which the wave function exits the potential barrier as shown in Fig. 1.

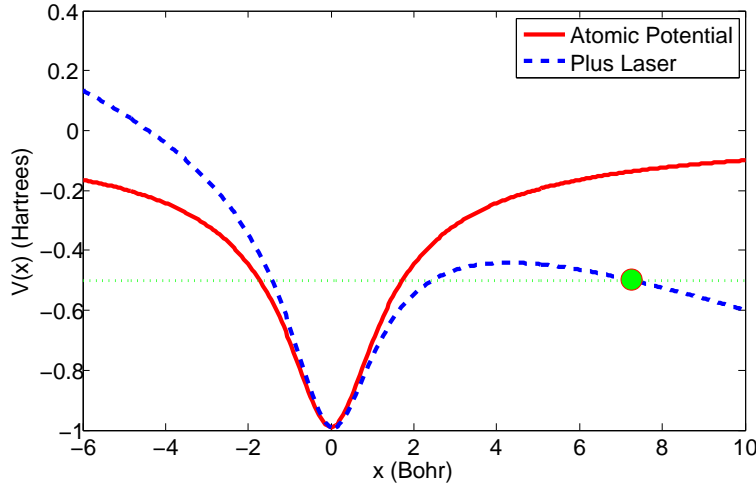


FIG. 1: Illustration of the tunneling barrier representing ionization of an atom in an intense laser field. The dashed curve shows the ionic potential plus the potential of the laser electric field. The fine dotted line at  $V(x) = -0.5$  represents the energy of the eigenstate. The ionic potential has been reduced by the laser field, allowing some of the bound electronic wave function at the origin to tunnel out into the continuum. With a classical model, tunneling cannot occur. Instead, the initial condition of the “tunnelled” electron is set at the exit of the classically forbidden region, marked by the circle.

For the initial position of the electron, we choose to place it at the point where it exits the classically forbidden tunnelling region. This position is commonly defined using a zero-range potential as  $x_0 = I_p/E_0$ , or using a Coulomb potential as

$$x_0 = \frac{I_p + \sqrt{I_p^2 - 4E_0 \cos(\omega t_0)}}{2E_0 \cos(\omega t_0)} \quad (1)$$

where  $I_p$  is the ionization energy,  $E_0$  is the peak electric field strength,  $\omega$  is the angular frequency of the laser field and  $t_0$  is the time of birth into the continuum. Electrons are given a zero initial velocity. These initial conditions are typical for semi-classical models [4, 8, 12, 14, 16, 21]. The electrons are propagated over a full cycle in the presence of the cosine laser field and a softened Coulomb potential by solving Newton’s equations using a

fourth order Runge-Kutta method. We use the softened potential

$$V(x) = -\frac{1}{\sqrt{x^2 + I_p^{-2}}} \quad (2)$$

so that the minimum value of the potential, at the origin, is  $-I_p$ . This form of softened potential is widely used across classical and semi-classical simulations [8, 25–28]. From the classical trajectories the time at which the electron returns to the origin and the kinetic energy at return can be determined, while the probability of a trajectory is determined via the ADK tunneling rate at the time of birth  $t_0$ . One-hundred and eight trajectories were sampled for each different intensity.

For the quantum simulations, we numerically solve the Schrödinger equation using the split operator method with the following Hamiltonian:

$$H(x, t) = \frac{-p^2}{2m} + V(x) + xE(t), \quad (3)$$

where  $V(x) = -\frac{1}{\sqrt{x^2 + \alpha^2}}$  with  $\alpha$  chosen such that the energy of the initial eigenstate of  $V(x)$  is  $-I_p$ , and the time dependent laser electric field (shown in Fig. 2) is defined as

$$E(t) = \begin{cases} E_0 \cos^2(\omega t), & t_s < t < 0 \\ E_0 \cos(\omega t), & 0 < t < t_f \end{cases}.$$

The cosine squared field is used for the initial quarter cycle in order to ensure a smooth turn on. Comparative simulations have been performed which show this does not effect the returning recollision energy or time significantly, but does decrease numerical artifacts. Simulations begin at  $t_s = -\frac{\pi}{2\omega}$  and end at  $t_f = \frac{5\pi}{2\omega}$ . The initial ground state wave function  $|\Psi(0)\rangle = |\Psi_g\rangle$  is the lowest eigenstate of the field-free potential  $V(x)$ . To isolate the recolliding trajectories, we define the continuum wavefunction  $|\Psi_c(t)\rangle$  by

$$|\Psi_c(t)\rangle = (1 - |\Psi_g\rangle\langle\Psi_g|)|\Psi(t)\rangle.$$

which is the full wavefunction minus the projection onto the bound state, in analogy with earlier studies isolating the recolliding wavepacket contribution [29]. We propagate the full wavefunction for the first half cycle, but at  $t = \frac{\pi}{2\omega}$  we remove the ground state and consider only the continuum wavefunction by using the projection operator considered above.

We employ a spatial window to isolate that portion of the continuum wave function near the origin, corresponding to the position of the ionic core. A window function is applied to the continuum wavefunction around the origin, and the resulting truncated wavefunction is Fourier-transformed to the momentum representation, i.e.

$$\Phi_R(p, t) = \int g(x) \Psi_c(x, t) e^{-ipx} dx$$

where  $g(x) = e^{-\frac{x^2}{2\sigma^2}}$ , and  $\sigma$  is chosen to cover the ground state wavefunction. In the results presented here,  $\sigma = \sqrt{10}$  a.u., and  $g(x)$  is truncated outside of  $x \in [-10, 10]$ . The window function and the initial ground state are shown in Fig. 3.

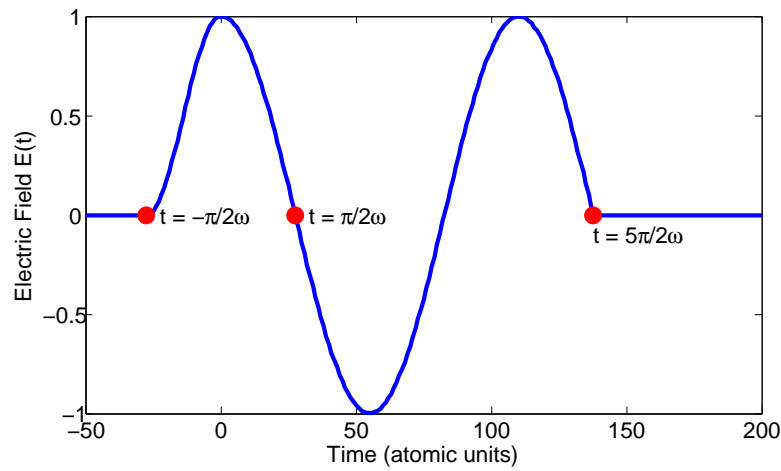


FIG. 2: Illustration of the laser electric field used in the quantum calculation. The first quarter-cycle has a smooth turn-on. At time  $t = \frac{\pi}{2\omega}$ , the bound state wave function is projected out to isolate the continuum portion of the wave function.

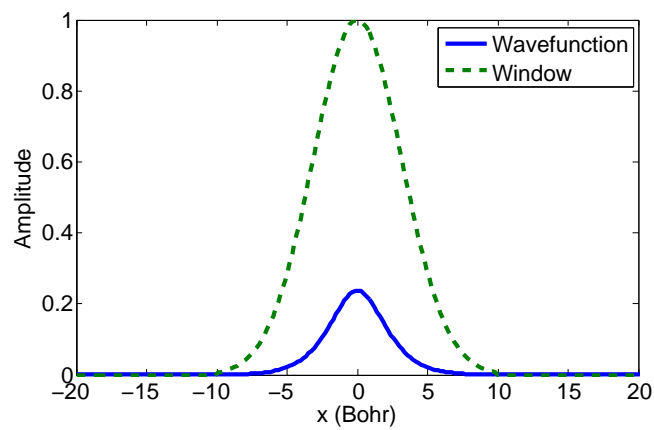


FIG. 3: Initial ground state wavefunction (solid line) and Fourier transform window (dashed line) in the spatial domain. The transform window is sufficiently broad to cover the ground state region without including significant continuum dynamics.

At this point the positive momentum components of the wavefunction are discarded, leaving only the trajectories which correspond to those turned by the laser field. From here the distribution of kinetic energies is calculated by applying the kinetic energy operator  $K = \frac{p^2}{2m}$ . By performing this algorithm for each time step, the recollision energy as a function of return time is mapped out. We are particularly interested in the mean energy as a function of time, as this should correspond to the classical trajectories in accordance with the Ehrenfest theorem.

### III. RESULTS

In order to compare the predictions of the two models, we first examine their results in a regime where both semi-classical methods and the canonical three step model are known to give accurate results. Figure 4 shows results obtained at a peak intensity of  $2.2 \times 10^{14}$  W/cm<sup>2</sup>, a wavelength of 800 nm, and  $I_p = 15.8$  eV, corresponding to argon and a Keldysh parameter of 0.77. The agreement between the mean recollision energy from the Schrödinger equation (in blue) and the Semi-classical Model (in green) is excellent for the long trajectories. Both predict a maximal return energy around the zero crossing of the field at  $270^\circ$ , and the two methods' prediction for maximal return energy of 62.5 eV is very close to the value of  $3.17U_p + 1.3I_p = 62.3$  eV determined from the more sophisticated fully quantum mechanical version of the three step model [30]. The most significant deviation is for the short trajectories in the semi-classical model; these trajectories are found to be born very far from the nucleus close to the field zero, and accelerated through the next subsequent half-cycle to recollide with high kinetic energy. While these trajectories have a vanishing probability relative to the long trajectories, they illustrate a potential problem with the semi-classical method which we shall see becomes significant at low intensities.

Figure 5 shows the maximum recollision energy as determined by the Schrödinger equation, semi-classical model and the canonical three step model. At high intensities, the agreement between all three models is excellent. The agreement applies even into the multiphoton regime and, for the Schrödinger equation and three step model, well into the over-barrier ionization regime (not shown), far beyond where the 3 step model might be thought to apply.

Below  $1 \times 10^{14}$  W/cm<sup>2</sup> however, the models begin to deviate severely. While the semi-classical model systematically over-estimates the return energy at all intensities, at lower field strengths the deviation becomes severe. In order to remove the influence of short trajectories with vanishing probabilities, we consider only return trajectories that have a relative probability of greater than  $10^{-6}$ . The results here are unchanged varying this cutoff up to  $10^{-3}$ . The increasing deviation at low intensities is due to the increasingly significant contribution from the short trajectories as the intensity becomes lower. An examination shows that while at high intensities a sharp cutoff in return energy can be seen, at low intensities the semi-classical model predicts a slow decrease in the probability of ever more energetic electrons. Below  $2 \times 10^{13}$  W/cm<sup>2</sup> no recollision is found to occur. Conversely, the full quantum treatment predicts lower return energies than the three step model at

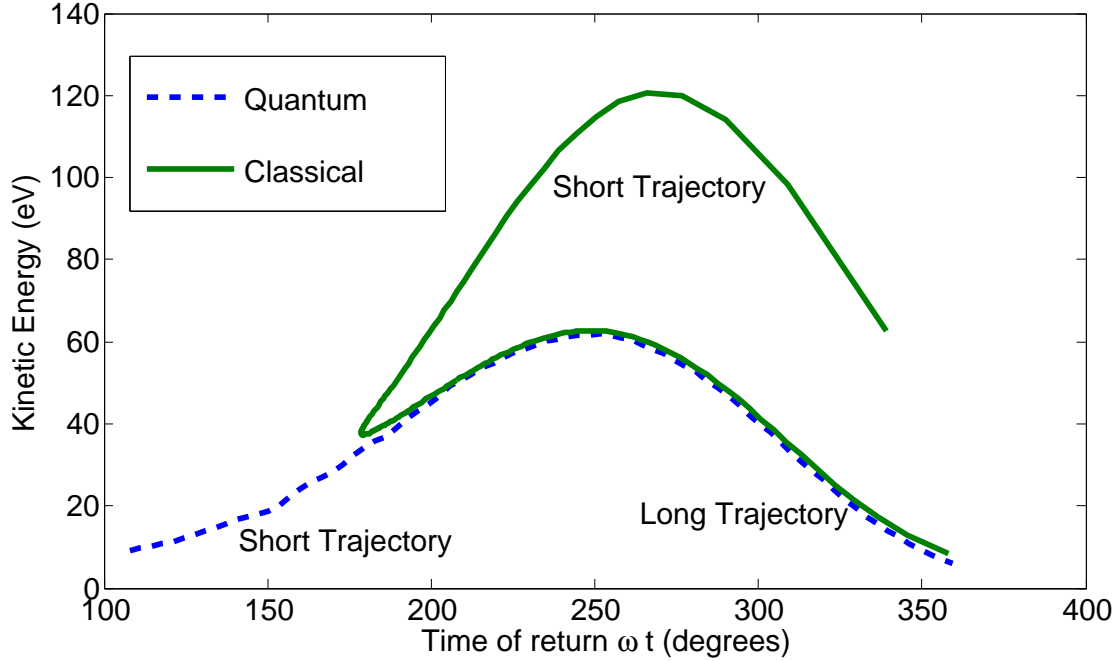


FIG. 4: The recollision energy vs. the time of return (given in units of  $\omega t$  and expressed in degrees) for the various models at an intensity of  $2.2 \times 10^{14}$  W/cm<sup>2</sup>. The dashed line shows the mean energy of the recolliding wavepacket from the 1D Schrödinger equation. The solid line shows the return energy from the semi-classical model. At this intensity, both models agree well with the canonical model, except for the low-probability short trajectories.

low intensities, as the increasingly weak field is no longer sufficient to draw the wavepacket away from the ionic core. The qualitatively different behaviour between the fully quantum mechanical and semi-classical calculations leads to the semi-classical model predicting a recollision energy 2.5 times that of the quantum case at the lowest intensities.

In addition to the semi-classical model incorrectly predicting the maximal return energy, at low intensities we also see a significant error in predictions of the return time. Figure 6 shows a comparison between energy vs. return time for the semi-classical model and the Schrödinger equation at a low intensity of  $6 \times 10^{13}$  W/cm<sup>2</sup>, a particularly interesting regime for NSDI where the recolliding electron is not expected to have sufficient energy to trigger a RESI process. We immediately see that while the Schrödinger equation predicts that short trajectories occur throughout the first half cycle after birth, the semi-classical model predicts all recollisions occur two half cycles after ionization, recolliding against the action of the field. Unlike at high intensities, the short trajectories now have comparable probability to the long trajectories in the semi-classical model. As time of birth is thought

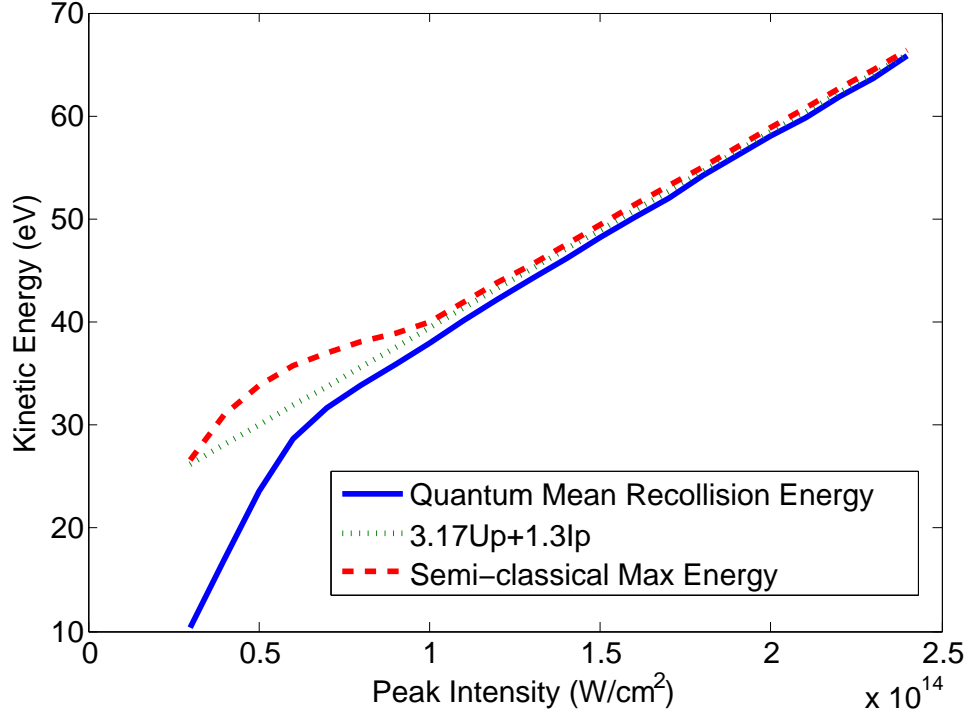


FIG. 5: The maximum recollision energy as a function of intensity given by canonical formula  $3.17U_p + 1.3I_p$ , full solution to the 1D Schrödinger equation and the semi-classical method. The agreement between the three models is excellent at high intensities but deviates at low intensities.

to be a major, if not primary determinant of the electron correlation in NSDI, this deviation suggests semi-classical methods might well break down completely at low intensities. These trajectories are now relegated to the third half cycle of the field by virtue of being born so far into the continuum that even acceleration through an entire half cycle is not sufficient to return them to the core within that half cycle. This error is thus attributable purely to the tunnelling step.

Another feature of the full Schrödinger equation solution which is not captured by the usual semi-classical method is the spread of energies in the recolliding wavepacket. For the semi-classical model, only a single kinetic energy is predicted, but the quantum model predicts a range of kinetic energies at any one time. In Fig. 7 we plot the standard deviation of the kinetic energy of the recolliding wavepacket, at its most energetic time of return, as a function of the intensity. The variance in the energy is seen to be quite significant, particularly at low intensities where only a few additional eV of energy might be necessary to allow the formation of doubly excited states or trigger a RESI process. Indeed we see that even at  $4 \times 10^{13} \text{ W/cm}^2$ , a simple estimate of the recollision energy as the mean plus the standard deviation gives 28.8 eV, enough to form a doubly excited state in argon [31].



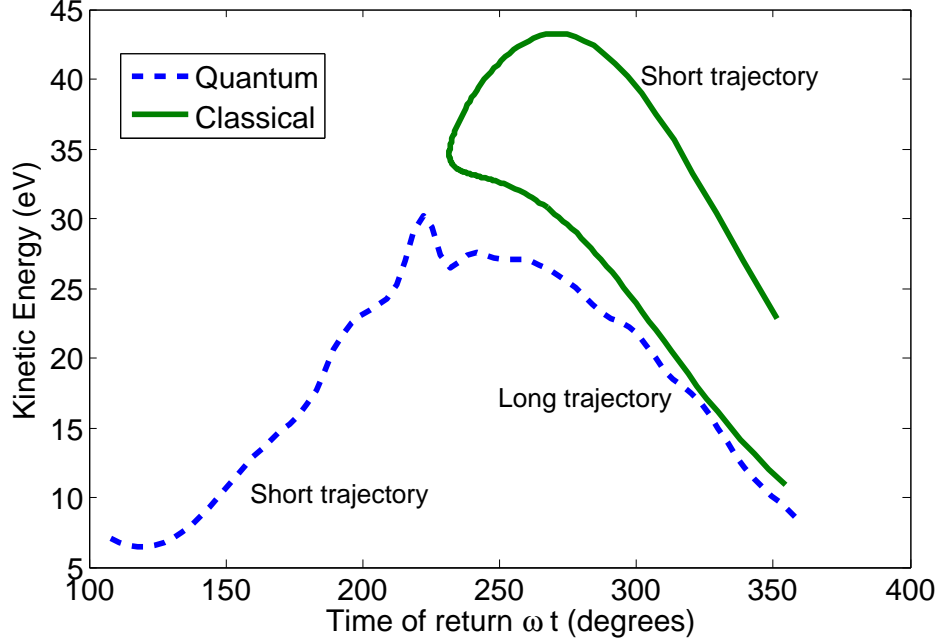


FIG. 6: The recollision energy vs. the time of recollision (given in phase of optical cycle in degrees) for the two models at an intensity of  $6 \times 10^{13} \text{ W/cm}^2$ . The dashed line shows the mean energy of the recolliding wavepacket from the 1D Schrödinger equation. The solid line shows the return energy from the semi-classical model. The two models now diverge heavily in terms of predicted return time as well as energy. Note that interference structures are also increasingly significant in the quantum model.

Modelling this spread in energies should be possible in semi-classical methods by sampling a variety of initial momenta parallel to the laser field.

#### IV. CONCLUSIONS

We have shown that semi-classical methods, widely used in analysing NSDI, deviate from a full quantum treatment in a variety of important ways. The semi-classical model systematically overestimates the recollision energy, with the deviation increasing at lower intensities. Furthermore, the semi-classical model, while correctly determining the recollision time at higher intensities, gives highly skewed results at lower intensities, and generally performs poorly handling the short trajectories. Finally, the semi-classical model as it is usually implemented does not capture the spread of energies seen in the quantum treat-

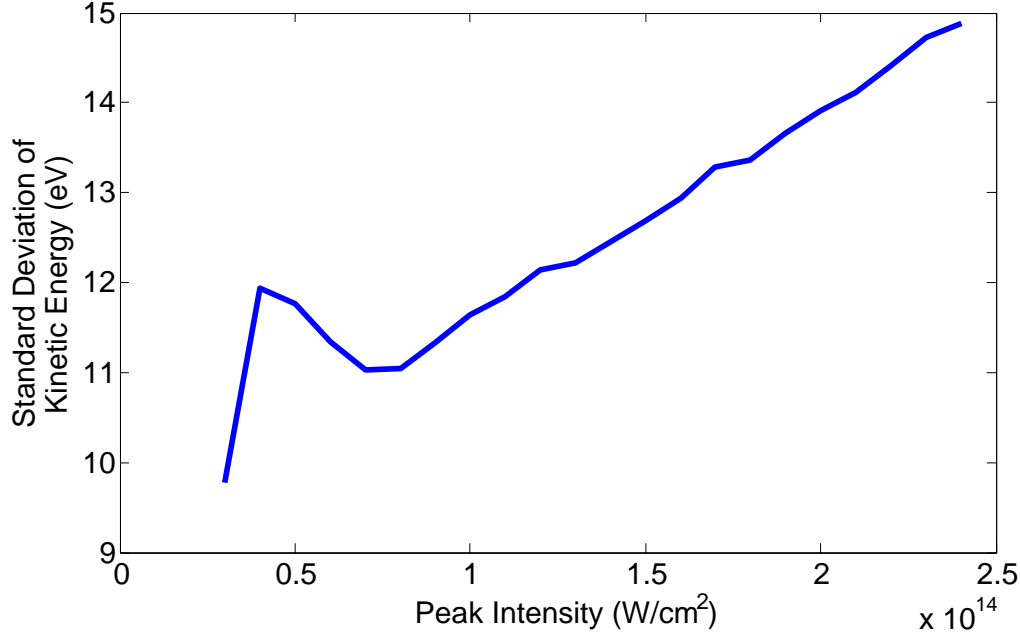


FIG. 7: The standard deviation of the distribution of kinetic energy of the recolliding wavepacket as a function of intensity. The standard deviation is taken at the time of recollision corresponding to the highest mean kinetic energy. As can be seen, there are significant energy contributions above the mean at all intensities.

ment. This spread of energies is quite significant, particularly at low intensities where the different NSDI mechanisms are expected to become very sensitive to the return energy. In particular this spread in energies can be expected to shift the cut-off for both knock-out collisions and RESI, as well as enable the formation of doubly excited states across all experimentally studied regimes. Our results point towards the necessity of quantum treatments at low intensities, as well as indicating that semi-classical methods should in future sample a variety of momenta parallel to the field at intermediate intensities in order to mimic the spread of return energies. At present the widely used semi-classical treatments risk giving incorrect results at intensities below the recollision knock-out regime.

## References

- [1] P. B. Corkum and F. Krausz, *Nature Physics* **3**, 381 (2007).
- [2] F. Krausz and M. Ivanov, *Reviews of Modern Physics* **81**, 163 (2009).

- [3] P. B. Corkum, *Physical Review Letters* **71**, 1994 (1994).
- [4] C. F. de Morisson Faria and X. Liu, *Journal of Modern Optics* **58**, 1076 (2011).
- [5] S. Larochelle, A. Talebpour, and S. L. Chin, *Journal of Physics B: Atomic, Molecular and Optical Physics* **31**, 1201 (1998).
- [6] A. Talebpour, C.-Y. Chien, Y. Liang, S. Larochelle, and S. L. Chin, *Journal of Physics B: Atomic, Molecular and Optical Physics* **30**, 1721 (1997).
- [7] B. Walker, B. Sheehy, L. F. DiMauro, P. Agostini, K. J. Schafer, and K. C. Kulander, *Phys. Rev. Lett.* **73**, 1227 (1994).
- [8] W. Becker, X. Liu, P. J. Ho, and J. H. Eberly, *Reviews of Modern Physics* **84**, 1011 (2012).
- [9] A. Staudte, C. Ruiz, M. Schöffler, S. Schössler, D. Zeidler, T. Weber, M. Meckel, D. Villeneuve, P. Corkum, A. Becker, et al., *Physical Review Letters* **99**, 1 (2007).
- [10] A. Rudenko, V. de Jesus, T. Ergler, K. Zrost, B. Feuerstein, C. Schröter, R. Moshhammer, and J. Ullrich, *Physical Review Letters* **99**, 263003 (2007).
- [11] A. Rudenko, K. Zrost, B. Feuerstein, V. de Jesus, C. Schröter, R. Moshhammer, and J. Ullrich, *Physical Review Letters* **93**, 253001 (2004).
- [12] B. Bergues, M. Kübel, N. G. Johnson, B. Fischer, N. Camus, K. J. Betsch, O. Herrwerth, A. Senftleben, a. M. Sayler, T. Rathje, et al., *Nature communications* **3**, 813 (2012).
- [13] M. Weckenbrock, D. Zeidler, a. Staudte, T. Weber, M. Schöffler, M. Meckel, S. Kammer, M. Smolarski, O. Jagutzki, V. Bhardwaj, et al., *Physical Review Letters* **92**, 213002 (2004).
- [14] N. Camus, B. Fischer, M. Kremer, V. Sharma, A. Rudenko, B. Bergues, M. Kübel, N. G. Johnson, M. F. Kling, T. Pfeifer, et al., *Physical Review Letters* **108**, 073003 (2012).
- [15] J. Parker, B. Doherty, K. Taylor, K. Schultz, C. Blaga, and L. DiMauro, *Physical Review Letters* **96**, 133001 (2006).
- [16] A. Emmanouilidou, J. S. Parker, L. R. Moore, and K. T. Taylor, *New Journal of Physics* **13**, 043001 (2011).
- [17] J. Chen and C. Nam, *Physical Review A* **66**, 053415 (2002).
- [18] A. Emmanouilidou and A. Staudte, *Physical Review A* **80**, 1 (2009).
- [19] Y. Liu, S. Tschuch, A. Rudenko, M. Dürr, M. Siegel, U. Morgner, R. Moshhammer, and J. Ullrich, *Physical Review Letters* **101**, 5 (2008).
- [20] Y. Liu, D. Ye, J. Liu, A. Rudenko, S. Tschuch, M. Dürr, M. Siegel, U. Morgner, Q. Gong, R. Moshhammer, et al., *Physical Review Letters* **104**, 1 (2010).
- [21] D. F. Ye and J. Liu, *Physical Review A* **81**, 1 (2010).
- [22] Y. Zhou, Q. Liao, and P. Lu, *Physical Review A* **80**, 19 (2009).
- [23] J. U. Brackbill and B. I. Cohen, eds., *Multiple Time Scales* (Academic, New York, 1985).
- [24] D. M. Villeneuve, M. Y. Ivanov, and P. B. Corkum, *Phys. Rev. A* **54**, 736 (1996).
- [25] G. Camiolo, G. Castiglia, P. Corso, E. Fiordilino, and J. Marangos, *Physical Review A* **79**, 1 (2009).
- [26] S. Sukiasyan, C. McDonald, C. Van Vlack, C. Destefani, T. Fennel, M. Ivanov, and T. Brabec, *Physical Review A* **80**, 1 (2009).
- [27] K. Shomsky, Z. Smith, and S. Haan, *Physical Review A* **79**, 1 (2009).
- [28] L. B. Fu, G. G. Xin, D. F. Ye, and J. Liu, *Physical Review Letters* **108**, 103601 (2012).
- [29] O. Smirnova, S. Patchkovskii, and M. Spanner, *Physical Review Letters* **98**, 123001 (2007).
- [30] M. Lewenstein, P. Balcou, M. Ivanov, and P. Corkum, *Physical Review A* **49**, 2117 (1994).
- [31] T. M. El Sherbini and S. H. Allam, *Annalen der Physik* **494**, 2 (1982).